



Clustering and synchronization of n Huygens' clocks

K. Czolczynski^a, P. Perlikowski^{a,b}, A. Stefanski^a, T. Kapitaniak^{a,*}

^a Division of Dynamics, Technical University of Lodz, Stefanowskiego 1/15, 90-924 Lodz, Poland

^b Institute of Mathematics, Humboldt University of Berlin, Unter der Linden 6, 10099 Berlin, Germany

ARTICLE INFO

Article history:

Received 30 June 2009

Received in revised form 5 August 2009

Available online 2 September 2009

Keywords:

Pendulum

Clocks

Synchronization

ABSTRACT

We study the synchronization of a number of pendulum clocks hanging from an elastically fixed horizontal beam. It has been shown that after a transient, different types of synchronization between pendulums can be observed: (i) the complete synchronization in which all pendulums behave identically, (ii) pendula create three or five clusters of synchronized pendulums, (iii) antiphase synchronization in pairs (for even n). We give evidence why the configurations with a different number of clusters are not observed. We argue that these phenomena are robust and can be observed experimentally.

© 2009 Elsevier B.V. All rights reserved.

1. Introduction

Over the last three decades the subject of the synchronization has attracted increasing attention from different fields [1–3]. The study of synchronization can be traced back to the works of the Dutch researcher Christian Huygens in XVIIth century [4]. He showed that a couple of mechanical clocks hanging from a common support were synchronized. Huygens had found that the pendulum clocks swung in exactly the same frequency and π out-of-phase, i.e., in antiphase synchronization. After the external perturbation, the antiphase state was restored within half an hour and remained indefinitely.

Recently, several research groups revisited the Huygens' experiment. Pogromsky et al. [5] designed a controller for synchronization problem for two pendula suspended on an elastically supported rigid beam. To explain Huygens' observations, Bennett et al. [6] built an experimental device consisting of two interacting pendulum clocks hanged on a heavy support which was mounted on a low-friction wheeled cart. The device moves by the action of the reaction forces generated by the swing of the two pendula and the interaction of the clocks occurs due to the motion of the clocks base. It has been shown that to repeat the results of Huygens, high precision (the precision that Huygens certainly could not achieve) is necessary.

Another device mimicking Huygens' clock experiment, the so-called "coupled pendula of the Kumamoto University" [7], consists of two pendula whose suspension rods are connected by a weak spring, and one of the pendula is excited by an external rotor. The numerical results of Fradkov and Andrievsky [8] show simultaneous approximate in-phase and antiphase synchronization. Both types of synchronization can be obtained for different initial conditions. Additionally it has been shown that for the small difference in the pendula frequencies they may not synchronize.

A very simple demonstration device was built by Pantaleone [9]. It consists of two metronomes located on a freely moving light wooden base. The base lies on two empty soda cans which smoothly rolls on the table. Both in-phase and antiphase synchronization of the metronomes have been observed.

The coupling in Huygens experiments [1,5–9] differs from the coupling described in most recent works as in this case one cannot explicitly identify neither the coupling structure nor the coupling coefficients. We call this type of coupling the

* Corresponding author.

E-mail address: tomaszka@p.lodz.pl (T. Kapitaniak).

coupling through elastic structure [10–12]. The coupling through elastic structure allows to investigate how the dynamics of the particular oscillator is influenced by the dynamics of other subsystems. An interaction mechanism between two oscillators leading to exact antiphase and in-phase synchronization has been described by Dilao [13]. It has been shown that if two coupled nonlinear oscillators reach the antiphase or the in-phase synchronization, the oscillations frequency is different from the frequency of the uncoupled oscillators. However, the precise dynamics of the n clocks hanging from the common support is unknown.

The large oscillations of London's Millennium Bridge on the day it was opened, have given another impulse to the studies of the dynamical behavior of the systems coupled by elastic structure. The assumption of the inseparability of the bridge wobbling and crowd synchrony allow to explain the behavior of Millennium Bridge [14,15].

In this paper we study a synchronization problem for n pendula hanging from an elastically fixed horizontal beam. Each pendulum performs a periodic motion which starts from different initial conditions. We show that after a transient different types of synchronization between pendula can be observed. The first type is in-phase complete synchronization (CS) in which all pendula behave identically. In the second type one can identify the groups (clusters) of synchronized pendula. We show that only configurations of three and five clusters are possible and derive algebraic equations for the phase difference between the pendula in different clusters. In the third type, which is possible only for even n , one observes antiphase synchronization in $n/2$ pairs of pendula. Besides these synchronized states it is possible to observe the uncorrelated motion of the pendula. We anticipate our assay to be a starting point for further studies of the synchronization and creation of the small-worlds [16–19] in the systems coupled by an elastic medium. For example, the behavior of the biological systems (groups of humans or animals) located on elastic structure could be investigated. In particular, a general mechanism for crowd synchrony can be identified.

The paper is organized as follows. In Section 2 we describe the action of the pendulum clock. Section 3 presents examples of experimental synchronization of metronomes. The theoretical model which explains the observed behavior is developed in Section 4. Section 5 presents the results of our numerical studies. Theoretical explanation of the existence of only three or five clusters of the synchronized pendula is given in Section 6. Finally, we summarize our results in Section 7.

2. Pendulum clocks

In the early-to-mid-14th century, large mechanical clocks began to appear in the towers of several large Italian cities. These clocks were weight-driven and regulated by a verge-and-foliot escapement [20]. This mechanism pre-dates the pendulum and was originally controlled by a foliot, a horizontal bar with a weight at each end. A vertical shaft (verge) is attached to the middle of the foliot and carries two small plates (pallets) sticking out like flags from a flag pole. One pallet is near the top of the verge and one near the bottom and looking end-on down the verge the pallets are a little over ninety degrees apart. The escape wheel is shaped somewhat like a crown and turns about a vertical axis. As the wheel tries to turn, one tooth of the wheel pushes against the upper pallet and starts the foliot moving. As the tooth pushes past the upper pallet, the lower pallet swings into the path of the escape wheel. The momentum of the moving foliot pushes the escape wheel backwards but eventually the system comes to rest. It is now the turn of the lower pallet to push the foliot and so on. The system has no natural frequency of oscillation – it is simply force pushing inertia around. Verge-and-foliot mechanisms reigned for more than 300 years with variations in the shape of the foliot. All had the same basic problem: the period of oscillation of this escapement depended heavily on the amount of driving force and the amount of friction in the drive and was difficult to regulate.

Another advance was the invention of spring-powered clocks between 1500 and 1510 by a German locksmith Peter Henlein. Replacing the heavy drive weights permitted smaller clocks. Although they slowed down as the mainspring unwound, they were popular among wealthy individuals due to their size and the fact that they could be put on a shelf or table instead of hanging from the wall.

The pendulum clock was invented in 1656 by Ch. Huygens, and patented the following year. He was inspired by investigations of pendulums by Galileo Galilei beginning around 1602. Galileo discovered the key property that makes pendulums useful timekeepers, i.e., isochronism, which means that the period of swing of a pendulum is approximately the same for different sized swings. The introduction of the pendulum, the first harmonic oscillator used in timekeeping, increased the accuracy of clocks enormously, from about 15 min per day to 15 s per day [20–22] leading to their rapid spread as existing 'verge-and-foliot' clocks were retrofitted with pendulums.

These early clocks, due to their verge escapements, had wide pendulum swings of up to 100° . Huygens discovered that wide swings made the pendulum inaccurate, causing its period, and thus the rate of the clock, to vary with unavoidable variations in the driving force provided by the movement. Clockmakers' realization that only pendulums with small swings of a few degrees are isochronous motivated the invention of the anchor escapement around 1670, which reduced the pendulum's swing to 4° – 6° [20]. In addition to increased accuracy, this allowed the clock's case to accommodate longer, slower pendulums, which needed less power and caused less wear on the movement.

All mechanical pendulum clocks have five basic parts: (i) a power source; either a weight on a cord that turns a pulley, or a spring, (ii) a gear train that steps up the speed of the power so that the pendulum can use it, (iii) an escapement that controls the speed and regularity of the pendulum. It transfers the energy stored in the spring to the motion of the pendulum by means of wheels, gears, and ratchets, i.e., it gives the pendulum precisely timed impulses to keep it swinging, and which releases the gear train wheels to move forward a fixed amount at each swing, (iv) the pendulum, a weight on a rod, (v) an

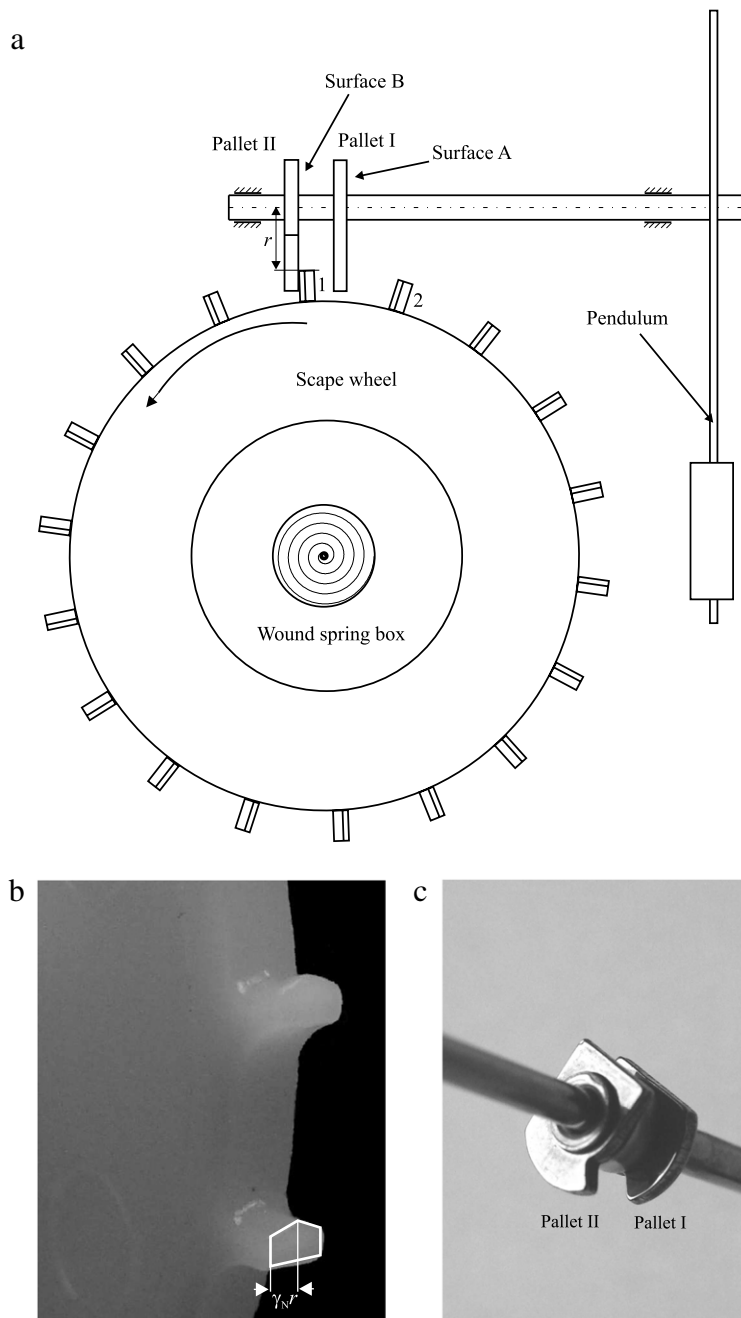


Fig. 1. Escapement mechanism of metronome; (a) scheme of the mechanism, (b) view of the scape wheel, (c) view of the anchor pallets.

indicator or dial that records how often the escapement has rotated and therefore how much time has passed, usually a traditional clock face with rotating hands.

Typical escapement mechanism is shown in Fig. 1(a–c). The oscillations of the considered clock pendulum are controlled by the anchor escapement mechanism shown in Fig. 1(a). It consists of the scape wheel (details are shown in Fig. 1(b)) and two anchor pallets mounted on the pendulum axis (details are shown in Fig. 1(c)). The energy is supplied by a wound spring connected with the scape wheel. The escapement mechanism acts as shown in Fig. 2(a–d). In the first stage one of the triangle shaped teeth of the scape wheel impacts the pallet I. For the angle of pendulum displacement $\phi_i < 0$ (Fig. 2(a)) surface A of the pallet I slides on the top edge of the triangle teeth 1 and excitation moment $M_i = 0$. In the case of $0 < \phi_i < \gamma_N$ (Fig. 2(b)) the edge of the pallet I is in contact with the side surface of the teeth 1 and the horizontal component of the reaction generates excitation moment M_N . When increasing ϕ_i passes critical value γ_N , pallet I slides off the teeth 1 and the second stage of the mechanism acting starts. The teeth 1 impacts on the pallet II. For $\phi_i > 0$ (Fig. 2(c)) surface B of the pallet

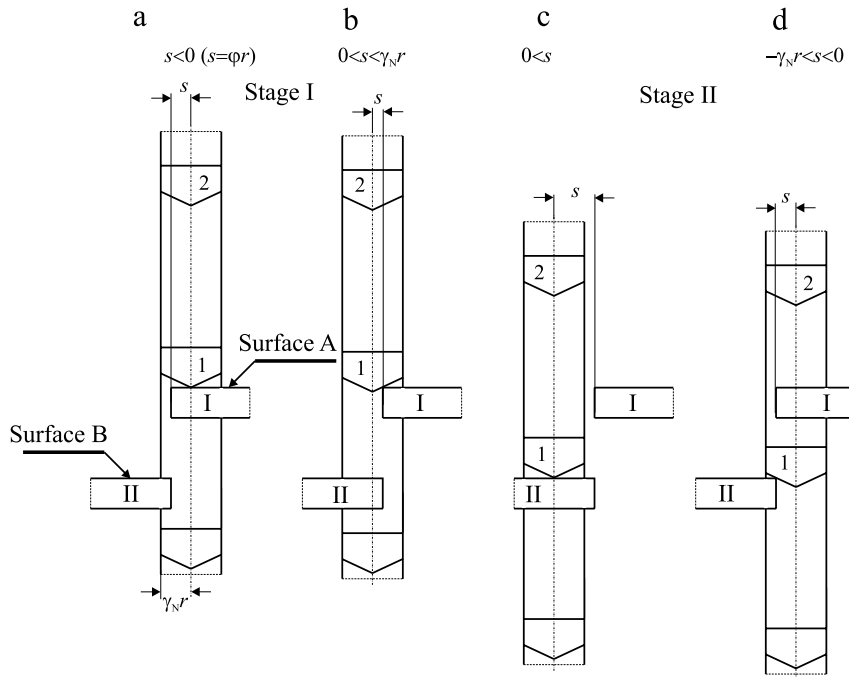


Fig. 2. Acting of the escapement mechanism.

II slides on the edge of the teeth 1 and no excitation moment is generated. When $-\gamma_N < \phi_i < 0$ (Fig. 2(d)) the edge of the pallet II is in contact with the side surface of the teeth 1 and the horizontal component of the reaction generates excitation moment $-M_N$. When ϕ_i exceeds the critical value $-\gamma_N$, i.e., $\phi_i < -\gamma_N$ the pallet II slides off the teeth 1. Next, the successive teeth 2 impacts pallet I and the first stage starts again.

3. Experimental synchronization of metronomes

In our experiments we observed oscillations of n metronomes (mass of each one 0.119 kg) located on a plate. The plate sits on the light polished rolls which can roll on the parallel smooth base and is connected by the spring to the vertical base. Metronomes are Wittner's Taktell-Piccolino (Series 890). The frequency of the metronome is adjusted by changing the position of a mass on the metronome's pendulum bob. The metronomes's standard settings range from 40 ticks per minute (largo) to 208 ticks per minute (prestissimo). For the performed measurements the highest standard frequency setting have been used. They corresponds to 104 oscillations per minute as the metronomes tick twice per cycle.

Pendulum metronomes act in the same way as pendulum clock. Energy is supplied to each metronome by a hand wound spring and their oscillations are controlled by the escapement mechanism as described in Fig. 2(a–c). The speed camera (Photron APX RS with the film speed at 1500 frames per second) has been used to observe the motion of the metronomes.

In the first case three metronomes have been located on the plate. Fig. 3 shows that metronomes perform steady state periodic oscillations with a constant phase difference $\Delta\beta = \beta_2 - \beta_1 = \beta_3 - \beta_2 = \beta_1 - \beta_3 = 2\pi/3$.

In Fig. 4(a,b) time series of 11 metronomes located on the elastic plate which can roll on the base are shown. N indicates a number of periods of oscillations, i.e., $t = 2N\pi/\alpha$. Fig. 4(a) presents five clusters symmetrical configuration ($n_I = 1$, $n_{II} = 4$, $n_{III} = 1$, $n_{IV} = 1$, and $n_V = 4$), and Fig. 4(b) three clusters symmetrical configuration with respectively $n_I = 1$, $n_{II} = 5$, and $n_{III} = 5$ pendula.

Generally, in case of the light base (mass 0.058 kg) with smooth surface we observe complete synchronization of all metronomes. In this case the damping in the system is very low and the metronomes; ticks destabilize antiphase synchronizations [9]. For more damped system (rough surface of a heavier base of the mass 2 kg) we observe: (i) pairs of metronomes synchronized in antiphase for even n and (ii) occurrence three of five clusters of synchronized metronomes.

4. The model

In our studies we consider a system shown in Fig. 5. The beam of mass M can move in the horizontal direction x with the viscous friction given by a damping coefficient c_x . One side of the beam is attached to the base through the spring with stiffness coefficient k_x . The beam supports n identical pendulum clocks with pendula of the length l and mass m . The position of the i -th pendula is given by a variable ϕ_i and its oscillations are damped by viscous friction described by

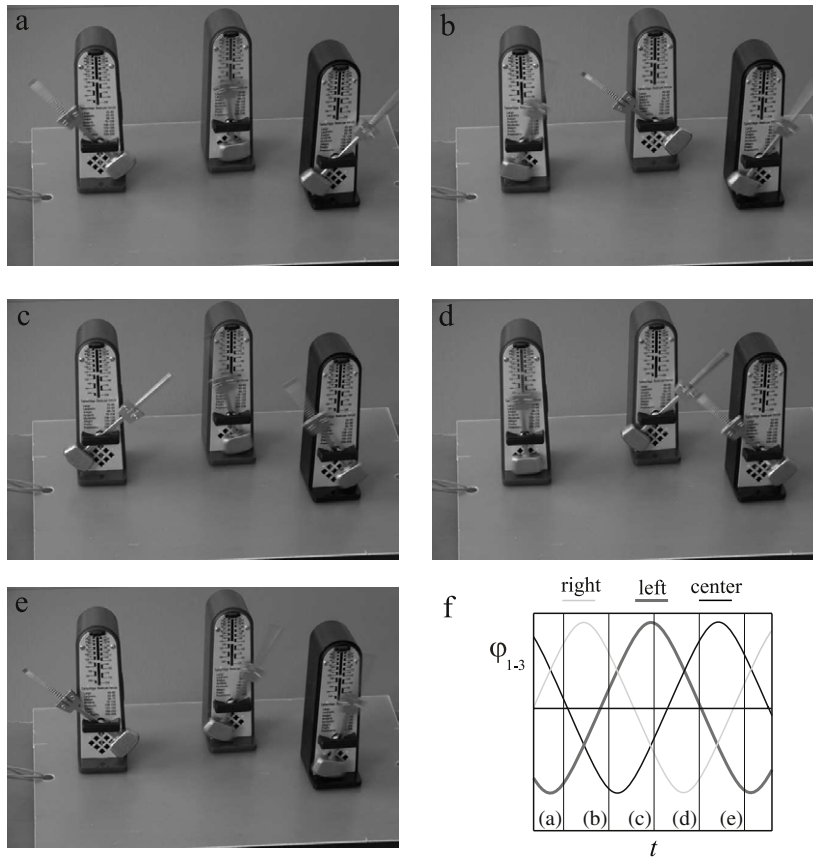


Fig. 3. Three metronomes located on the plate which can roll on the base obtain a synchronous state with a phase difference $\Delta\beta = \beta_2 - \beta_1 = \beta_3 - \beta_2 = \beta_1 - \beta_3 = 2\pi/3$.

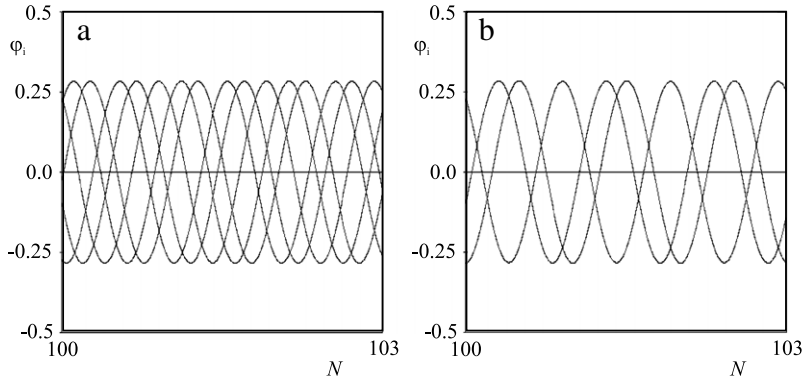


Fig. 4. Time series of 11 metronomes located on the plate which can roll on the base; N indicates a number of periods of oscillations ($t = 2N\pi/\alpha$): (a) five clusters configuration, $\beta_{II} = 0.475\pi$, $\beta_{III} = 0.791\pi$, (b) three clusters configuration, $\beta_{II} = 0.53\pi$.

damping coefficient c_ϕ . The beam is considered as a rigid body so the elastic waves along it are not considered. We describe phenomena which take place far below the resonances for both longitudinal and transverse oscillations of the beam.

The system equations can be written in a form of Euler–Lagrange equations:

$$ml^2\ddot{\phi}_i + c_\phi\dot{\phi}_i + m\ddot{x}l \cos \phi_i + mgl \sin \phi_i = M_i, \tag{1}$$

$$(M + nm)\ddot{x} + \sum_{i=1}^n (ml\ddot{\phi}_i \cos \phi_i - ml\dot{\phi}_i^2 \sin \phi_i) + c_x\dot{x} + k_x x = 0, \tag{2}$$

where g is a gravitational acceleration. The clock escapement mechanism (described in Appendix) represented by momentum M_i provides the energy needed to compensate the energy dissipation due to the viscous friction c_ϕ and to keep

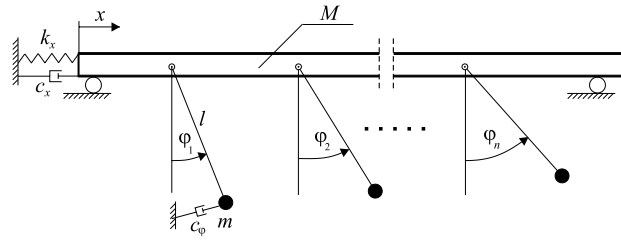


Fig. 5. The model of n pendula hanging from an elastic horizontal beam.

the clock running [23]. This mechanism acts in two successive steps (the first step is followed by the second one and the second one by the first one). In the first step if $0 < \phi_i < \gamma_N$ then $M_i = M_N$ and when $\phi_i < 0$ then $M_i = 0$, where γ_N and M_N are constant values which characterize the mechanism. For the second stage one has for $-\gamma_N < \phi_i < 0$ $M_i = -M_N$ and for $\phi_i > 0$ $M_i = 0$. Under these assumptions dynamics of the pendulum clock is described by a self-excited oscillator with a limit cycle [21,24] (see also Refs. [7–9]). Particularly, we consider escapement mechanism which is used in metronomes. In Ref. [9] it has been shown that the metronome can be described by self-excited van der Pol oscillator.

After the initial transient the pendula perform the periodic oscillations so the solution of Eq. (1) can be approximately described as:

$$\phi_i = \Phi \sin(\alpha t + \beta_i), \quad (3)$$

where Φ , α , β_i are respectively the amplitude, the frequency and the phase difference. As all pendula are the same so Φ and α are the same for each of them. The oscillations of the pendula differ only by the phase difference β_i .

It should be mentioned here that our theoretical results are based on the approximation of the pendula motion given by Eq. (5). In numerical simulations of Eq. (1)–(2) we got: $\phi_i = 0.144 \sin(\alpha t + \beta_i) + 0.0033 \sin 3(\alpha t + \beta_i) + 6.75 \cdot 10^{-4} \sin 5(\alpha t + \beta_i) + 3.2 \cdot 10^{-4} \sin 7(\alpha t + \beta_i) + \dots$ which clearly shows that the higher harmonics are small and have small (negligible) influence on the system (1,2) motion.

To study the stability of the solution of Eq. (1)–(2) we add perturbations δ_i and σ to the variables ϕ_i and x and obtain the following linearized variational equation:

$$ml^2 \ddot{\delta}_i + m\ddot{\sigma} l \cos \phi_i + ml\delta_i(g \cos \phi_i - \ddot{x} \sin \phi_i) + c_\phi \dot{\delta}_i = 0, \\ (M + nm)\ddot{\sigma} + \sum_{i=1}^n (m\ddot{\delta}_i \cos \phi_i - ml\dot{\phi}_i^2 \delta_i \cos \phi_i - ml\ddot{\phi}_i \sin \phi_i - 2ml\dot{\phi}_i \dot{\delta}_i \sin \phi_i) + c_x \dot{\sigma} + k_x \sigma = 0. \quad (4)$$

The solution of the Eq. (1)–(2) given by $\phi_i(t)$ and $x(t)$ is stable when the solution of Eq. (3) δ_i and σ tend to zero for $t \rightarrow \infty$.

In our numerical simulations we consider $m = 1$, $l = g/4\pi^2$, and $c_\phi = 0.01$ so the frequency of pendula oscillations α is equal to 2π . The stiffness k_x and damping c_x coefficients are assumed to be proportional to the beam mass M . The clock mechanism parameters are assumed to be $M_N = 0.075$ and $\gamma_N = \pi/36$. We assume that the initial conditions for the pendula are given by the initial value of β_{i0} , i.e., $\phi_{i0} = \Phi \sin \beta_{i0}$ and $\dot{\phi}_{i0} = \alpha \Phi \cos \beta_{i0}$. For the given parameters of the pendula and the clock mechanism $\Phi = 0.3$

5. Results

5.1. Three pendula ($n = 3$)

In Fig. 6 we plot the position of each pendulum given by Eqs. (1) and (2) in the phase space $\phi_i, \alpha \dot{\phi}_i$ at the time when the first pendulum is moving through the equilibrium position $\phi_1 = 0$ with the positive velocity $\dot{\phi}_1 > 0$. The points indicate the transients leading from the given initial conditions to the final configuration indicated in bold. After the initial transients the pendula perform periodic oscillations (which are visible in Fig. 6 by a single point for each pendulum) with the same amplitude (as the distance of each point to the origin (0, 0) is equal). The oscillations of the pendula differ only by the phase differences β_i .

Fig. 6(a,b) shows two possible configurations for the system (1,2) with three pendula. In the first configuration (shown in Fig. 6(a)) there is a constant phase difference $\Delta\beta = \beta_2 - \beta_1 = \beta_3 - \beta_2 = \beta_1 - \beta_3 = 2\pi/3$ between the pendula. We call this configuration a symmetrical synchronization (SS). In Fig. 6(b) one observes complete synchronization (CS). Besides these configurations we observed also the desynchronous behavior (DSB) of all pendula. In DSB regime the phase difference between pendula is not constant and is changing chaotically. All observed steady states are stable as the solution of the variational equation (3) decays. They can be observed in a wide range of the control parameters M and k_x as shown in Fig. 7, where SS, CS and DSB are indicated respectively in black, white and grey colors. In the calculation shown in Fig. 7 we assumed the following initial conditions $\beta_{10} = 0$, $\beta_{20} = \pi/8$, $\beta_{30} = \pi/9$, $x_0 = \dot{x}_0 = 0$.

In Fig. 8 we present the basins of attraction of the possible steady states of the system (1) in the $\beta_{20} - \beta_{30}$ plane, where β_{20} and β_{30} represent the initial positions of the second and the third pendula. Other initial conditions have been assumed

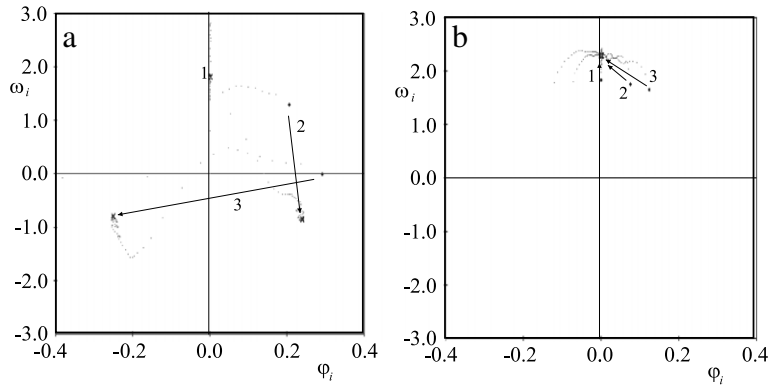


Fig. 6. The synchronization configurations for three pendula; $m = 1, l = g/4\pi^2, c_\phi = 0.01, M = 1, c_x = 0.1M, k_x = M, M_N = 0.075, \gamma_N = \pi/36$: (a) symmetrical synchronization with phase difference $\Delta\beta = 2\pi/3; \beta_{10} = 0, \beta_{20} = 2\pi/8, \beta_{30} = 2\pi/4$ (b) CS; $\beta_{10} = 0, \beta_{20} = 2\pi/24, \beta_{30} = 2\pi/18$.

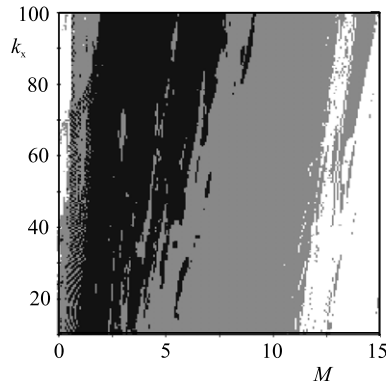


Fig. 7. The steady states of Eqs. (1) and (2) for different values of parameters M and k_x ; $m = 1, l = g/4\pi^2, c_\phi = 0.01, c_x = 0.1M, M_N = 0.075, \gamma_N = \pi/36, \beta_{10} = 0, \beta_{20} = \pi/8, \beta_{30} = \pi/9, x_0 = \dot{x}_0 = 0$. SS, CS and DSB are indicated respectively in black, white and grey colors.

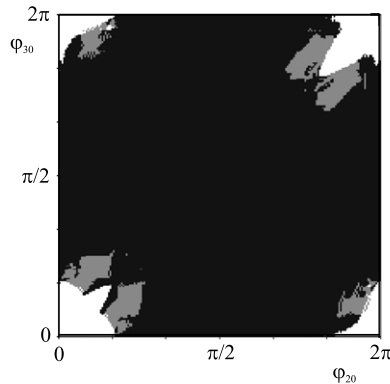


Fig. 8. The basins of attraction of the possible steady states of Eqs. (1), (2) in the ϕ_{20} – ϕ_{30} plane; $m = 1, l = g/4\pi^2, c_\phi = 0.01, M = 1, c_x = 0.1M, k_x = M, M_N = 0.075, \gamma_N = \pi/36, \beta_{10} = 0, x_0 = \dot{x}_0 = 0$. The basins of SS, CS and DSB are indicated respectively in black, white and grey colors..

to be equal to zero, i.e., $\beta_1 = 0, x_0 = \dot{x}_0 = 0$. The basins of SS, CS and DSB are indicated respectively in black, white and grey colors.

5.2. n pendula ($n > 3$)

In what follows, we show the examples of typical configurations in the system of more than 3 pendula.

Fig. 9(a–c) shows three possible configurations for the system (1,2) with six pendula. The points indicate the transients leading from the given initial conditions to the final configuration indicated in bold. In the first configuration (shown in

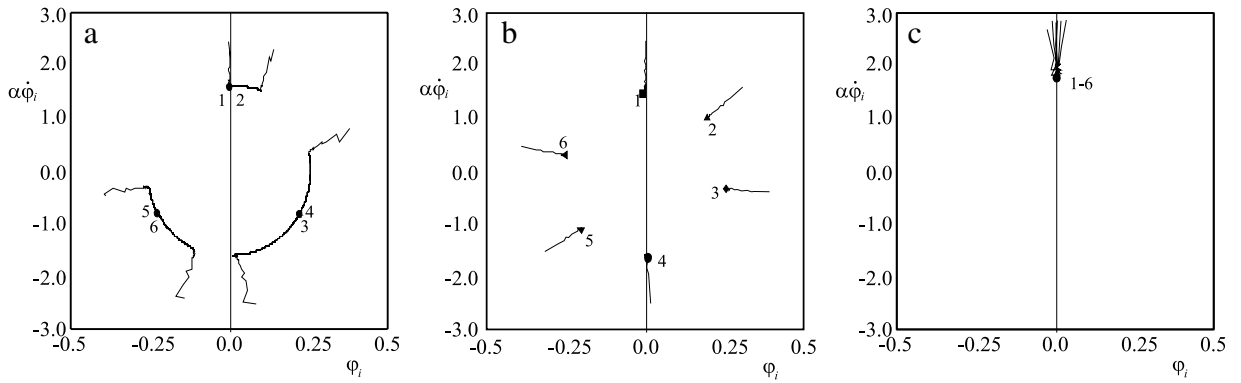


Fig. 9. The synchronization configurations for six pendula; $m = 1$, $l = g/4\pi^2$, $c_\phi = 0.01$, $M = 1$, $c_x = 0.1M$, $k_x = M$, $M_N = 0.075$, $\gamma_N = \pi/36$: (a) symmetrical synchronization of three clusters of two synchronized pendula, phase difference between clusters $\Delta\beta = 2\pi/3$; $\beta_{10} = \pi/6$, $\beta_{20} = 1.27\pi$, $\beta_{30} = 0.27\pi$, $\beta_{40} = 1.29\pi$, $\beta_{50} = 0.55\pi$, $\beta_{60} = 1.61\pi$, $x_0 = \dot{x}_0 = 0$, (b) three pairs of pendula synchronized in antiphase; $\beta_{10} = 0$, $\beta_{20} = 1.01\pi$, $\beta_{30} = 0.27\pi$, $\beta_{40} = 1.29\pi$, $\beta_{50} = 0.55\pi$, $\beta_{60} = 1.56\pi$, $x_0 = \dot{x}_0 = 0$, (c) CS; $\beta_{10} = \pi/6$, $\beta_{20} = 0.173\pi$, $\beta_{30} = 0.167\pi/9$, $\beta_{40} = 0.187\pi$, $\beta_{50} = 0.161\pi$, $\beta_{60} = 0.157\pi$, $x_0 = \dot{x}_0 = 0$.

Fig. 9(a) there are three clusters (pendula 1, 2, 3, 4 and 5, 6) of two synchronized pendula. The phase difference between the pendula in different clusters is equal to $\Delta\beta = 2\pi/3$ between the pendula. Three pairs of pendula synchronized in antiphase (the phase difference between pendula in each pair is equal to $\Delta\beta = \pi$) are shown in **Fig. 9(b)**. Pendula 1, 2 and 3 are respectively in antiphase with pendula 4, 5 and 6. The phase difference between pendula in different pairs depends on the initial conditions. In **Fig. 9(c)** one observes complete synchronization (CS). For even n we have not observed (DSB) of all pendula.

In **Fig. 10(a–d)** we plot the position of each of $n = 11$ pendula in the phase space $\phi_i, \dot{\alpha}\phi_i$ at the time when the first pendulum is moving through the equilibrium position $\phi_1 = 0$ with the positive velocity $\dot{\phi}_1 > 0$. **Fig. 10(a)** shows the configuration of three clusters with respectively $n_I = 2$, $n_{II} = 4$, and $n_{III} = 5$ pendula. The pendula in each cluster are synchronized. **Fig. 10(b)** shows the configuration with five clusters of respectively $n_I = 1$, $n_{II} = 3$, $n_{III} = 2$, $n_{IV} = 1$, and $n_V = 4$ pendula. In **Fig. 10(c)** the special case of the symmetrical three clusters configuration with respectively $n_I = 1$, $n_{II} = 5$, and $n_{III} = 5$ pendula is shown. **Fig. 10(d)** presents the symmetrical configuration of five clusters ($n_I = 1$, $n_{II} = 4$, $n_{III} = 1$, $n_{IV} = 1$, and $n_V = 4$).

For all considered odd n besides the above configurations we have observed; (i) a complete synchronization, (ii) desynchronous behavior of all pendula. For even n additionally; (iii) the antiphase synchronization in pairs have been observed. In the considered range of n we have not observed other stable cluster configuration.

6. Discussion

6.1. Influence of the beam motion on the pendula oscillations

The synchronization between the pendula can be obtained as a result of the interplay between the period of oscillations of the pendula, the amplitude of the beam oscillations and the phase difference between the motions of the pendula and the beam. In the simplest example of one pendulum hanging from the beam, the beam motion which is in-phase (out-of-phase) with motion of the pendulum increases (decreases) the period of oscillations of the pendulum. In the case of n pendula hanging from the beam, the beam motion can temporarily increase or decrease their period of oscillations allowing synchronization. One should notice here that the described mechanism explains why it is impossible to observe the existence of two groups of pendula with unequal number of members which synchronize in antiphase, i.e., due to the unequal total mass of the pendula in each group the influence of the beam motion on each group cannot be the same.

To give an explanation why only three and five cluster configurations are observed we consider a horizontal displacement of the beam Under the assumption (3) Eq. (1) can be linearized to the following form

$$(M + nm)\ddot{x} + c_x\dot{x} + k_x x = \sum_{i=1}^n (-m\ddot{\phi}_i + m\dot{\phi}_i^2 \phi_i). \quad (5)$$

Substituting Eq. (2) in Eq. (5) and taking into consideration the relation $\cos^2 \alpha \sin \alpha = 1/4(\sin \alpha + 3 \sin 3\alpha)$ one gets

$$(M + nm)\ddot{x} + c_x\dot{x} + k_x x = \sum_{i=1}^n \left(m\alpha^2 \Phi \sin(\alpha t + \beta_i) + \frac{1}{4} m\alpha^2 \Phi^3 (\sin(\alpha t + \beta_i) + 3 \sin 3(\alpha t + \beta_i)) \right). \quad (6)$$

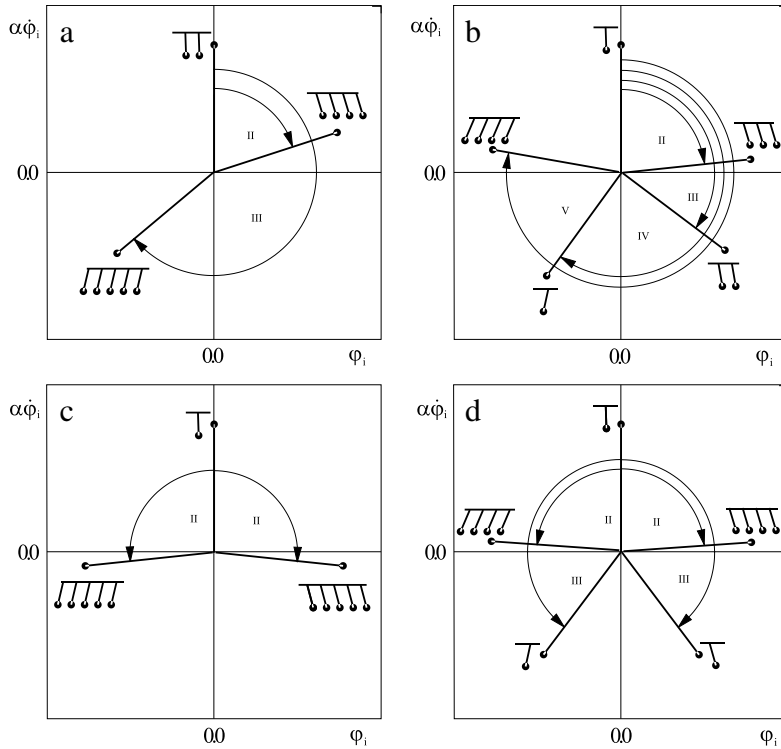


Fig. 10. Cluster configurations for $n = 11$ pendula; $m = 1, l = g/4\pi^2, c_\phi = 0.01, M = 1, c_x = 0.1M, k_x = M, M_N = 0.075, \gamma_N = \pi/36$: (a) three cluster configuration; $n_I = 2, n_{II} = 4, n_{III} = 5$, (b) five cluster configuration; $n_I = 1, n_{II} = 3, n_{III} = 2, n_{IV} = 1, n_V = 4$, (c) symmetrical three cluster configuration; $n_I = 1, n_{II} = 5, n_{III} = 5$, (d) symmetrical five cluster configuration; $n_I = 1, n_{II} = 4, n_{III} = 1, n_{IV} = 1, n_V = 4$.

The stationary solution $x_s(t)$ of Eq. (6) can be expressed in the form

$$x_s(t) = A_1 \sum_{i=1}^n \sin(\alpha t + \beta_i + \rho_1) + A_3 \sum_{i=1}^n \sin 3(\alpha t + \beta_i + \rho_3) \tag{7}$$

where A_1, A_3, ρ_1 and ρ_3 are constant.¹

Besides the local minimum for the $n/2$ pairs of pendula synchronized in antiphase (for even n) energy $x_s(t)$ given by Eq. (7) has local minima in two cases; (i) when the sum of the first harmonic components is equal to zero, (ii) when the sum of the first and the third harmonic components is equal to zero.

One can show that the conditions (i) and (ii) guarantee the local minima of energy of the undamped and non-excited system. Neglecting damping and excitation in Eqs. (1) and (2), i.e., assuming that $c_\phi \phi_i = M_i$ and $c_x = 0$ one can express a total energy of the system (1,2)

$$E = E_p + E_x = \frac{m}{2} \sum_{i=1}^n (\dot{x}^2 + l^2 \dot{\phi}_i^2 + 2\dot{x}\dot{\phi}_i l \cos \phi_i) + \frac{M\dot{x}^2}{2} + mgl \sum_{i=1}^n (1 - \cos \phi_i) + \frac{kx^2}{2}, \tag{8}$$

where E_p and E_x represent respectively the energy of n pendula and the energy of the motion in x direction.

Under the assumption (3) the energy of n pendula E_p is the same for all pendula configurations. Eqs. (2) and (7) allows us to write the energy of the motion in the direction x as follows

$$\begin{aligned} E_x &= \frac{1}{2}(M + nm)\dot{x}_s^2(t) + \frac{1}{2}k_x x_s^2(t) \\ &= \frac{1}{2}(M + nm) \left(\alpha A_1 \sum_{i=1}^n \cos(\alpha t + \beta_i) + 3\alpha A_3 \sum_{i=1}^n \cos 3(\alpha t + \beta_i) \right)^2 \\ &\quad + \frac{1}{2}k_x \left(A_1 \sum_{i=1}^n \sin(\alpha t + \beta_i) + A_3 \sum_{i=1}^n \sin 3(\alpha t + \beta_i) \right)^2. \end{aligned} \tag{9}$$

One can notice that for $c_x = 0$ the constants ρ_1 and ρ_3 in Eq. (7) are equal to zero.

¹ The exact formulas for the parameters A_1, A_3 and ρ can be found in any textbook on the theory of linear oscillations, e.g. J.J. Thomsen, *Vibrations and Stability; Order and Chaos*, (McGraw Hill, London 1997).

Local minima of Eq. (9) for the cases (i) and (ii) are clearly visible. It is possible to show that the first case occurs for three cluster configuration and the second one for five cluster configuration. The lack of other harmonics components in Eq. (7) and (9) shows why the configurations with a number of clusters different from 3 or 5 are not observed.

6.2. Three cluster configuration

Consider three cluster configuration with respectively n_I , n_{II} and n_{III} ($n_I \leq n_{II} \leq n_{III}$) pendula in the successive cluster. The sum of the first harmonic components in Eq. (9) is equal to zero when the angles β_{II} and β_{III} fulfill the relation:

$$\begin{aligned} n_I + n_{II} \cos \beta_{II} + n_{III} \cos \beta_{III} &= 0, \\ n_{II} \sin \beta_{II} + n_{III} \sin \beta_{III} &= 0. \end{aligned} \quad (10)$$

The solution of Eq. (10) exists when $n_I + n_{II} \leq n_{III}$. In the symmetrical case $n_{II} = n_{III}$ and $\beta_{III} = 2\pi - \beta_{II}$ Eq. (10) reduces to

$$\cos \beta_{II} = \frac{-n_I}{2n_{II}}, \quad (11)$$

for which the solution exists if $n_I \leq 2n_{II}$. Our numerical and experimental results show that in the case of three cluster configuration clock oscillate with the frequency larger than the frequency of uncoupled clock. We observed $\alpha \approx 2\pi + 0.034$.

6.3. Five cluster configuration

Five cluster configuration with respectively n_I , n_{II} , n_{III} , n_{IV} and n_V pendula in the successive cluster exists when the sums of the first and the third harmonics components in Eq. (9) are equal to zero. In this case, it is possible to show that the angles β_{II-V} fulfill the relation:

$$\begin{aligned} n_I + n_{II} \cos \beta_{II} + n_{III} \cos \beta_{III} + n_{IV} \cos \beta_{IV} + n_V \cos \beta_V &= 0, \\ n_{II} \sin \beta_{II} + n_{III} \sin \beta_{III} + n_{IV} \sin \beta_{IV} + n_V \sin \beta_V &= 0, \\ n_I + n_{II} \cos 3\beta_{II} + n_{III} \cos 3\beta_{III} + n_{IV} \cos 3\beta_{IV} + n_V \cos 3\beta_V &= 0, \\ n_{II} \sin 3\beta_{II} + n_{III} \sin 3\beta_{III} + n_{IV} \sin 3\beta_{IV} + n_V \sin 3\beta_V &= 0. \end{aligned} \quad (12)$$

In the symmetrical cluster configuration $n_{II} = n_{IV}$, $n_{III} = n_V$, $\beta_{II} = 2\pi - \beta_{IV}$, $\beta_{III} = 2\pi - \beta_V$ Eq. (12) reduce to

$$\begin{aligned} n_I + 2n_{II} \cos \beta_{II} + 2n_{III} \cos \beta_{III} &= 0, \\ n_I + 2n_{II} \cos 3\beta_{II} + 2n_{III} \cos 3\beta_{III} &= 0. \end{aligned} \quad (13)$$

In five cluster configuration the displacement of the beam $x_s(t)$ (given by Eq. (7)) and energy E_x (given by Eq. (9)) are equal to zero, i.e., in the linear approximation of system (1,2) beam is in rest. In the numerical studies of the Eq. (1), (2) we have observed very small oscillations of the beam which are due to the nonlinear terms (omitted in Eq. (7)) and the acting of the escapement mechanism. In the case of five cluster configuration all pendula oscillate with the frequency nearly equal to the frequency of uncoupled clock. In our numerical and experimental show that $\alpha \approx 2\pi + 0.0001$.

7. Conclusions

To summarize, we have studied the phenomenon of the synchronization in the array of the pendulum clocks hanging from an elastically fixed horizontal beam. We show that besides the complete synchronization of all pendulum clocks and creation of the pairs of the pendulum clocks synchronized in antiphase (for even n), the pendula can be grouped either in three or five clusters only. The pendula in the clusters perform complete synchronization and the clusters are in the form of the phase synchronization characterized by a constant phase difference between the pendula given by Eqs. (10)–(13).

We give evidence that the observed behavior is robust in the phase space and can be observed in real experimental systems. The clustering in three or five clusters is possible for any number of pendulum clock n if the solution of Eq. (10) or Eq. (12) exists. In the considered range of $n \leq 30$ the solution of at least one of these equations exists. It should be mentioned here that it is easier to observe clustering phenomena for odd number of pendulum clocks. For even number of clock clustering is theoretically possible, but the basin of attraction of this configuration is much smaller than the basin of attraction of the configuration which consists of the pair of clocks synchronized in antiphase.

In the considered case we show that the clocks clustering phenomena take place far below the resonances for both longitudinal and transverse oscillations of the beam when the displacements of the beam are very small. We can add that the similar phenomena have been observed in the system of n pendula hanging from the string in which transversal and longitudinal oscillations of the string are considered. These results will be reported elsewhere [23].

Acknowledgement

This study has been supported by the Polish Department for Scientific Research (DBN) under project No. N501 033 31/2490.

References

- [1] A. Pikovsky, M. Resenblum, J. Kurths, *Synchronization: A Universal Concept in Nonlinear Sciences*, Cambridge University Press, Cambridge, 2001.
- [2] I.I. Blekham, *Synchronization in Science and Technology*, ASME, New York, 1988.
- [3] S. Boccaletti, J. Kurths, D. Osipov, D.L. Valladares, C.S. Zhou, *Phys. Rep.* 366 (2002) 1.
- [4] C. Huguenii, *Horoloqium Oscilatorium*, Apud F. Muquet, Parisiis, 1673, English translation: *The Pendulum Clock*, Iowa State University Press, Ames, 1986.
- [5] A.Yu. Pogromsky, V.N. Belykh, H. Nijmeijer, Controlled synchronization of pendula, in: *Proceedings of the 42nd IEEE Conference on Design and Control*, Maui, Hawaii, 2003, pp. 4381–4385.
- [6] M. Bennet, M.F. Schatz, H. Rockwood, K. Wiesenfeld, *Proc. R. Soc. Lond. A* 458 (2002) 563–579.
- [7] M. Kumon, R. Washizaki, J. Sato, R.K.I. Mizumoto, Z. Iwai, Controlled synchronization of two 1-DOF coupled oscillators, in: *Proceedings of the 15th IFAC World Congress*, Barcelona, 2002.
- [8] A.L. Fradkov, B. Andrievsky, *Internat. J. Non-linear Mech.* 42 (2007) 895.
- [9] J. Pantaleone, *Amer. J. Phys.* 70 (2002) 992.
- [10] K. Czolczynski, T. Kapitaniak, P. Perlikowski, A. Stefanski, *Chaos Solitons Fractals* 32 (2007) 920–926.
- [11] K. Czolczynski, P. Perlikowski, A. Stefanski, T. Kapitaniak, *Chaos Solitons Fractals* 32 (2007) 937–943.
- [12] K. Czolczynski, A. Stefanski, P. Perlikowski, T. Kapitaniak, *J. Sound Vibration* 322 (2009) 513.
- [13] R. Dilao, *Chaos* 19 (2009) 023118.
- [14] S.H. Strogatz, D.M. Abrams, A. McRobie, B. Eckhard, E. Ott, *Nature* 438 (2005) 43.
- [15] M.M. Abdulrehem, E. Ott, *Chaos* 19 (2009) 013129.
- [16] D.J. Watts, S.H. Strogatz, *Nature* 393 (1998) 440–442.
- [17] S.H. Strogatz, *Nature* 410 (2001) 268.
- [18] M. Barahona, L.M. Pecora, *Phys. Rev. Lett.* 89 (2002) 054101.
- [19] T. Nishikawa, A.E. Motter, Y.-C. Lai, F.C. Hoppensteadt, *Phys. Rev. Lett.* 91 (2003) 014101.
- [20] A.L. Rowlings, *The Science of Clocks and Watches*, Pitman, New York, 1944.
- [21] F.C. Moon, P.D. Stiefel, *Phil. Trans. R. Soc. A* 364 (2006) 2539.
- [22] M. Headrick, *IEEE Control Syst. Mag.* 22 (2002) 41.
- [23] K. Czolczynski, P. Perlikowski, A. Stefanski, T. Kapitaniak, (in preparation).
- [24] A. Andronov, A. Witt, S. Khaikin, *Theory of Oscillations*, Pergamon, Oxford, 1966.